

Aerodynamic Performance of Purge Flow Endwall Cooling in High Pressure Turbine Cascade

W Ghopa Wan Aizon^{1,2}, Ken-ichiFunazaki¹, TakemitsuMiura¹

¹Department of Mechanical System Engineering
University of Iwate

Morioka 020-8551 Iwate, Japan

Phone: +8119-6216423, FAX: +8119-6216423, E-mail: wanaizon@gmail.com

²National University of Malaysia

ABSTRACT

The endwall and blade film cooling systems are the typical solution adopted within gas turbines to allow further increase of turbine inlet temperature, avoiding critical material thermal stresses. Due to complex secondary flow field in the blade passage, endwall is more difficult to cool than blade surfaces. In the matter of fact, in endwall film cooling studies, it is necessary to investigate the interaction between coolant air and the secondary flow. In present study, the flow field of high-pressure turbine cascade has been investigated by 5-holes pitot tube to reveal the secondary flows behavior under the influenced of purge flows which is located $0.63C_{ax}$ upstream of blade leading edge. Experimental has significantly captured the effect of leakage air to secondary flows at blade downstream plane. Furthermore, numerical simulation had presented almost the same result where the presence of additional losses can be observed especially at higher MFR.

NOMENCLATURE

C	: chord length (0.0122m)
C_{ax}	: axial chord length of blade (0.0623m)
Q	: volume flow rate
m	: mass flow rate
U_{in}	: inlet velocity
U_z	: axial velocity
ρ	: density
n	: number of pitch
P_s	: static pressure
P_d	: dynamic pressure
P_{ti}	: inlet total pressure
P_{to}	: outlet total pressure
A	: duct section area
p	: cascade pitch
s	: blade span height
y	: pitchwise direction
z	: spanwise direction
SS	: suction surface
PS	: pressure surface

Subscript

∞	: main flow
2	: secondary air

Abbreviation

MFR	: mass flow ratio = $(\rho Q)_2 / (\rho Q)_\infty$
C_{pt}	: total pressure loss coefficient = $(P_{ti} - P_{to}) / (1/2) \rho U_{in}^2$

INTRODUCTION

In order to improve the efficiency of modern gas turbine engines, high-pressure turbine stage inlet temperature has been increased. Temperature increase cannot exceed the threshold level imposed by the metal temperature capability avoiding critical material stresses. The extremely high turbine inlet temperature requires the development of more sophisticated cooling designs for the material protection purpose, this not only for the airfoil section but also the endwall section of HP turbine nozzle. However, in high pressure turbine nozzle, the endwall region is considerably more difficult to cool than the blade aerofoil surfaces because of the complex secondary flow structure in the blade passage. The earliest contribution to the endwall flow field was made by Blair (1974), in which he clarified that vertical structures such as horse-shoe or passage vortex had a dominant impact on the heat transfer of film-cooled endwall. This also was proved by Takeshi et al. (1990) when he found a reduction of the endwall film cooling effectiveness near the blade leading edge due to the presence of the horse-shoe vortex. According to Fig. 1, the horseshoe vortex splits into suction and pressure side legs where the pressure side legs develops into passage vortex resulting strong cross passage pressure gradient. These vertical structures and their interaction which is generally called secondary flows are responsible for aerodynamic losses in the cascade. In film cooling study, the aerodynamic interaction of the cooling flows with the secondary flow field need to be verified in obtaining a higher cooling performance with a less effect to the turbine efficiency. The study related to the secondary flows on the endwall also done by Goldstein and Spores (1988), Kang and Thole (1999), Langston (1977), Sieverding (1984) and Wang et. al (1995). Kost and Nicklas (2001) presented aerodynamic measurement from a transonic cascade with an upstream leakage ejection located at $0.2C_{ax}$. They found that injection at this location promoted the separation and enhanced the vortex. Kost and Mullaert (2006) continued the study by moved the slot location to $0.3C_{ax}$ upstream of the cascade. From the results obtained, they found that the slot flow stayed closer to the endwall and provided better cooling than flow from slot located at $0.2C_{ax}$ of cascade upstream. Rehder and Dannhauer (2007), carried out the experimental studies to reveal the effects of injection flow angle from the upstream clearance of the linear cascade of LPT stator vanes. They observed that the leakage ejection perpendicular to the main flow direction amplifies the secondary flow, in particular the horseshoe vortex and

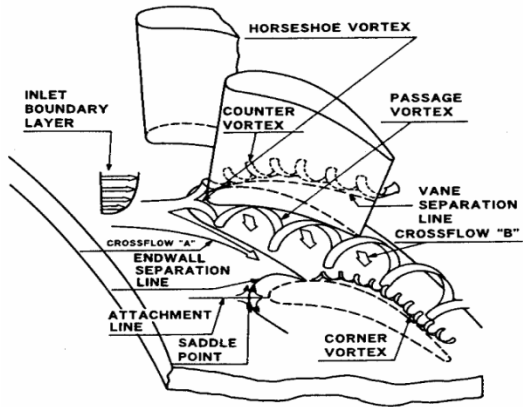


Fig. 1 Endwall secondary flow model (Takeishi et al, 1990)

therefore increases the secondary losses near the endwall region, whereas tangential leakage ejection causes significant reduction of this vortex system at the same time the secondary losses decrease at cascade exit. The presence of the gap and the flow through it within the passage can also affect the boundary layers and may induce additional secondary flows and vortex structures in the passage near the endwall. The upstream leakage studies were also done by other researchers such as Piggush and Simon (2007), Lynch and Thole (2008) and etc. The upstream leakage studies were also done by other researchers but currently still lack of information. Hence, studies on various test conditions are required to have detailed information on related study. Based on above literatures, it is clear that cooling air injection from upstream slot highly influenced the aerodynamics performance of turbine cascade. Furthermore, slot location and geometry as well as cooling air amount need to be carefully considered in film cooling studies. In present works, a new model with slightly higher aspect ratio compared with previous test blade has been designed. The slot location also was moved away from the blade leading edge. The study focuses on the aerodynamics effect of upstream leakage ejection on the secondary flow field. Aerodynamic measurements were performed by the use of pneumatic 5-holes Pitot tube to measure a total pressure at blade downstream. The flow field was also predicted by a numerical simulation using ANSYS CFX to enhance the understanding of flow field over the endwall especially at the region which cannot be obtained merely by the experimental. Based on the result obtained, total pressure loss and flow vorticity were determined and discussed.

EXPERIMENTAL PROCEDURES

The experimental investigations were conducted in the aerospace laboratory at Iwate University. Fig.2 shows the test apparatus used in this study, indicating main blower, diffuser, settling chamber, contraction nozzle. Secondary blower works to supply the secondary air into the plenum chamber which is attached at the bottom side of the test section. Then, a secondary air from the plenum chamber will be ejected to the mainstream through the leakage slot. A laminar flow meter was used to measure the mass flow rate of secondary air. Since this study focuses on aerodynamics behaviour, the secondary air was supplied without any heating. Measurement plane and slot geometry are shown in Fig. 3. The leakage slot was located $0.63C_{ax}$ upstream of the blade leading edge. The slot extended about 4 pitches and the width was $0.064C_{ax}$. In consideration of the plate thickness, normal injection into the main flow was highly expected in this study. All components of the test section except the test cascade were made of acrylic-resin plate in order to keep visibility from outside. The test cascade consisted of 2 segments, each of which had two identical HP turbine nozzle vanes, and two dummy vanes. The vane segments were produced by a rapid prototyping method using UV light hardening technique. An

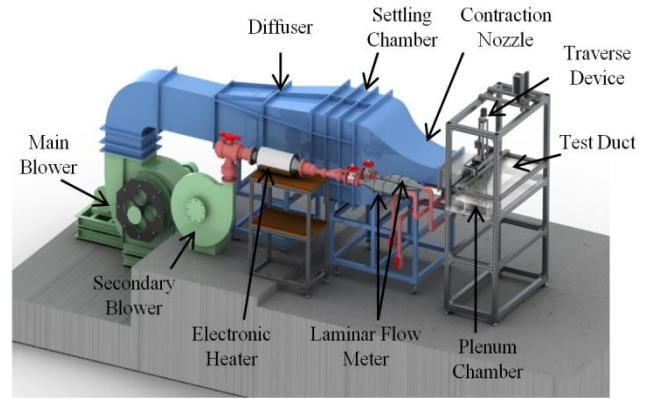


Fig.2 Overview of the test apparatus

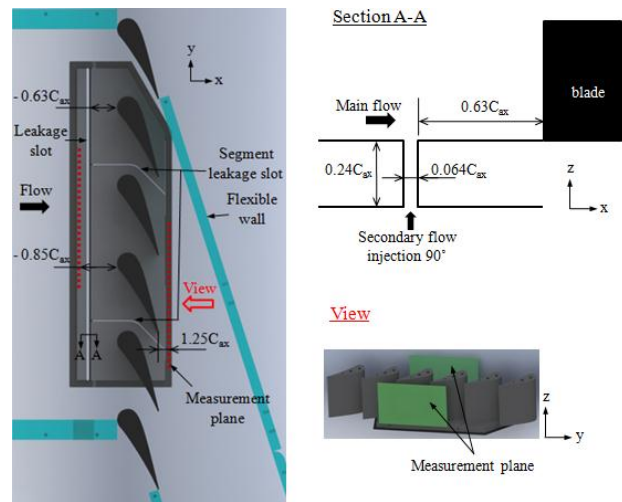


Fig. 3 Measurement area and slot geometry

L-type miniature pitot tube was placed upstream of the model-leading edge for inlet flow velocity measurement. The measurement system is constituted by pneumatic 5-holes Pitot tube, traverse device, pressure transducer and data logger which are connected to the computer for data collection. The flow field measurement at inlet has been conducted at the first in order to ensure uniform main flow distribution entering the cascade. Pneumatic 5-holes Pitot tube measurements have been performed at $0.85C_{ax}$ upstream plane. Based on the result obtained, the detail measurements of flow behaviour at $1.25C_{ax}$ downstream of blade leading edge were done. The location of those traverse plane are also shown in Fig. 2. In order to study effect of the upstream leakage ejection, two MFR of 1.2% and 2.2%, respectively were ejected to the main stream. However, the measurement without any leakage was firstly carried out to observe a baseline condition of flow field at blade downstream plane. For no leakage ejection case, a measurement was conducted without supplying a secondary air, therefore a flat endwall platform without slot was placed at the first to avoid a flow that coming from the high pressure main stream moving into the slot. The measurements at downstream plane were done by two phases where the first phase was to investigate a periodicity of flow at cascade outlet. 1200 points of measurement were started from the blade tip which traversing for 2 pitches and ended close to the endwall. On the other hand, second phase measurement were surveyed with a finer grid for only 1 pitch and a measurement started at midspan. The finest grid was 1mm and coarsest was 10mm with a 1120 points of measurement. Furthermore, the finer grid was adopted near the region where the blade wakes are expected. This plane has been surveyed by

means of 28 traverses in the pitchwise direction, each of them constituted by 40 measuring points spaced with variable steps which have a finer grid near the endwall. For each measuring point 10 samples have been collected and the pressures were calculated as time-averaged components. However, results based on finer grid measurements only will be presented in this paper. The head diameter of probe was 2.1mm and the nearest distance of measurement from the endwall was 2mm. The main flows Reynolds number of 1.25×10^5 was fixed throughout all test cases. This Reynolds number was determined based on blade chord length. Fig. 2 also indicates the viewpoint definition of all contours presented in this paper.

COMPUTATIONAL PROCEDURES

Fig. 4 illustrates the geometry of the model whereas Fig. 5 shows the mesh structures of the model. The computational domain consisted of the plenum chamber, 1 pitch endwall with a single blade periodicity channel designed by slot upstream the vane. The computational mesh system was created using Gridgen (Pointwise) with a fully structured model. This is a multiblocks meshing method which consisted of 10 structured blocks. The density of mesh cells is increased in the vicinity of the bottom, the top and the blade surfaces but also at injection location. The height of wall-adjacent cells in these regions is 0.02mm with the objective to obtain y^+ value close to 1 along the walls according to the applied Reynolds Number in this study. The entire computational domain comprises a total of 5.1 million hexahedral cells. To evaluate the grid independence of the solution, three others meshes have been tested with, 7.0 million, 9.2 and 14 millions of cells. A numerical prediction was adopted by commercial software; ANSYS CFX 12 and a very popular SST turbulence model were employed. Domain extended from $2.0C_{ax}$ upstream of the leading edge to $2.0C_{ax}$ downstream of the trailing edge. The boundary conditions are defined in accordance with the measurement conditions in the linear cascade facility located in Iwate University. Translational periodic boundary condition was applied on the pitchwise direction. Uniform distributions of measured stagnation pressure and static temperature were specified on the inlet boundary, while total mass flow rate including the leakage flow rate was given on the outlet boundary. As for the secondary flow, the measured mass flow rate and static temperature were specified on the entry plane of the plenum chamber. Non-slip and adiabatic conditions were given on the wall surface.

RESULT AND DISCUSSIONS

Baseline performance

Fig. 6 presents the aerodynamic performance at blade downstream for the baseline condition obtained by the EFD (a) compared with the SST (b). Top side of the figures illustrate the C_{pt} while bottom side showing the flow vorticity at the same plane of measurement. Based on EFD, losses at blade downstream are significantly influenced by blade wake and another two loss cores which are located at $y/p=0.45$, $z/s=0.09$ and close to endwall, $y/p=0.43$, respectively. The first core can be considered is associated with the passage vortex near the blade suction side while the second core is associated with interaction between wall boundary layer, wake profile and corner vortex coming from upstream. The vorticity contour gives a details information on the flow structures at this plane. The positive vorticity region rotating in clockwise direction illustrates the presence of passage vortex which has contributed to the highest losses. SST has over predicted the losses for the whole major loss regions. However, it also predicted that the pick of the losses was caused by the vorticity core which is associated by the passage vortex. Prediction illustrates slightly higher loss region compared with EFD at $y/p=0.8$. This predicted loss probably influenced by the SS horse-shoe vortex rotating in opposite direction with passage vortex. Since this is a lower region compared to

major losses, EFD could not significantly captured this region

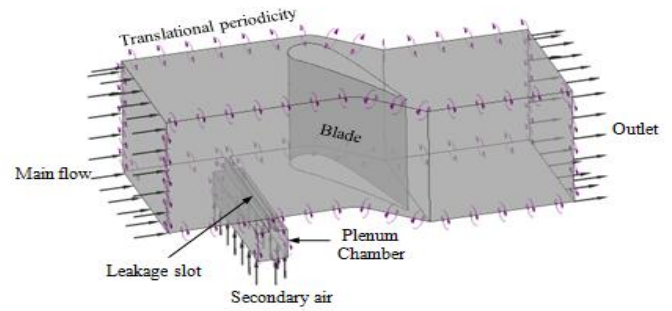


Fig. 4 Geometry of the model

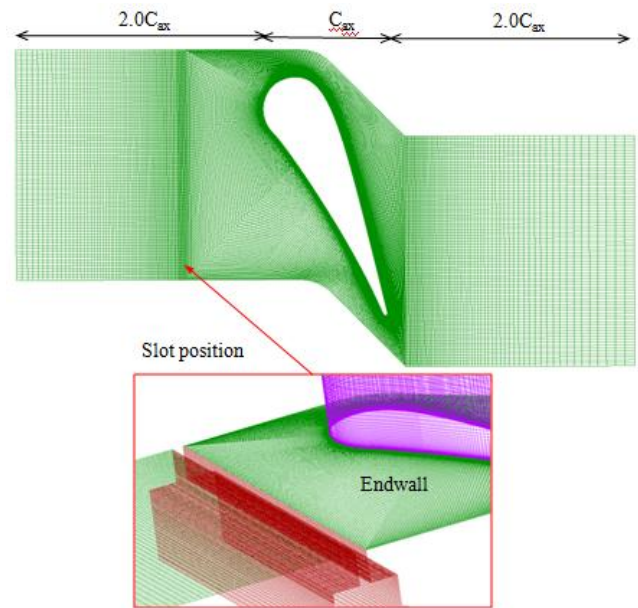


Fig. 5 Mesh structures for leakage ejection case

might be due to the low measurement resolution at this region.

Aerodynamics effects by upstream leakage ejection

The effect of the upstream leakage ejection can be observed in following contours. Two different ejections MFR of 1.2% and 2.2% have been tested and their results are shown in Fig. 6 and Fig. 7, respectively. Upstream leakage ejection seems to give several effects on the secondary flow at both MFR. For 1.2% of MFR, the shape of first loss core was changed and slightly moves towards midspan. This phenomenon could obviously be seen when increasing the injection amount to MFR=2.2%. The centre of the core became the highest in span direction compared with previous cases. Furthermore, the other side of the core was also being pulled to the right side and the presence of additional loss region have been captured. In both ejection cases. The higher the injection amount, the wider region of loss could be observed on the right side of the first core. This new loss region tends to become wider in pitchwise than the spanwise span direction. As shown in vorticity contours, compared to the baseline condition, the positive vorticity core were increased their strength and the position of the core region slightly shifted to the right side in pitchwise direction. Based on this phenomenon, the strength of passage vortex has been amplified after the injection which then promoted to the additional loss. The second loss core located close to the endwall region was also being affected. At higher MFR, the existence of this core could clearly be

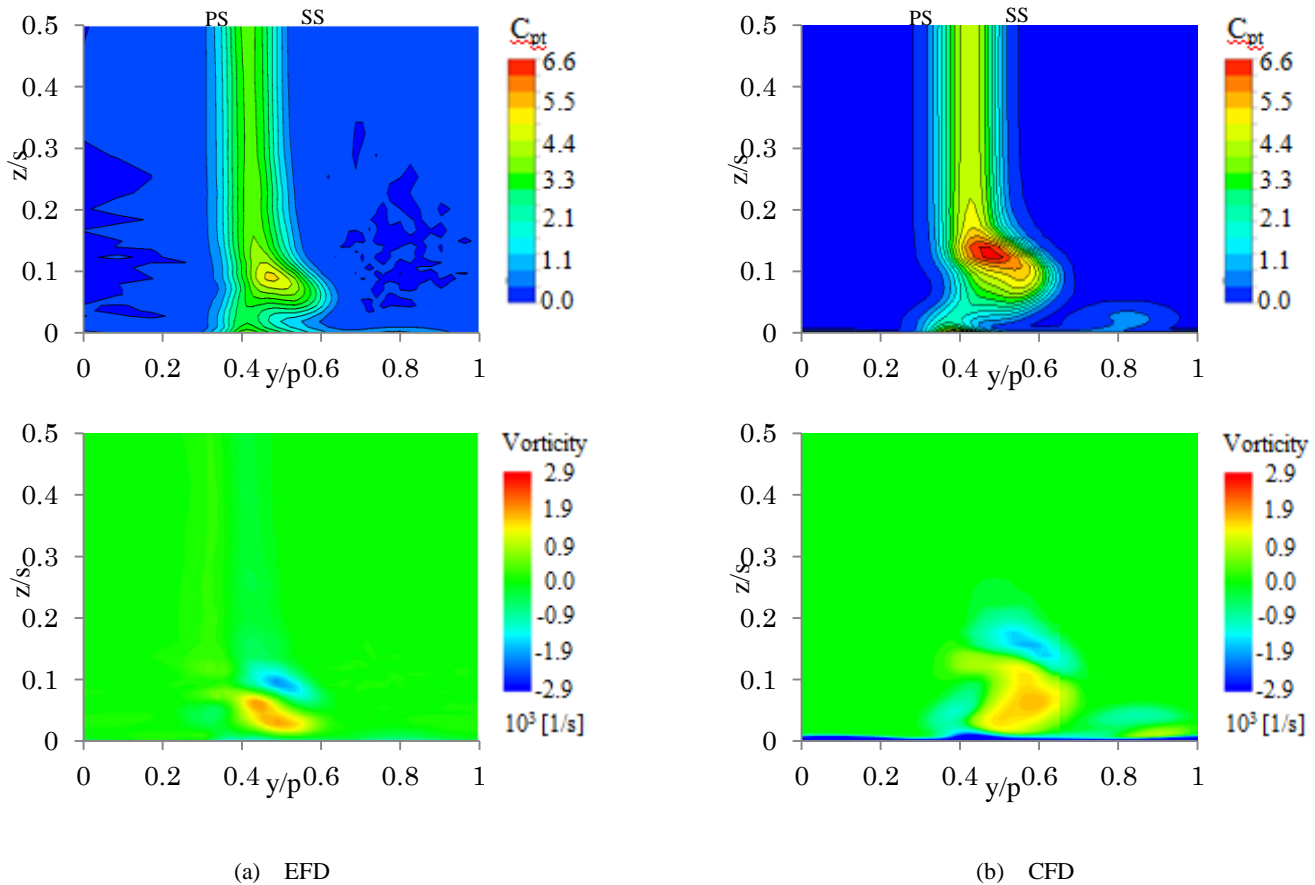


Fig. 6 Baseline condition- Total pressure loss and vorticity

observed. According to the negative vorticity region which is rotating in anticlockwise direction close to the endwall region, showing the increased strength of the corner vortex. The corner vortex was responsible to the change of second loss core. A similar trend of contours was obtained by the CFD simulation. Almost the same shape of the first loss core was predicted in both ejection cases. The centre of the core also slightly moved upward as been captured in EFD when the MFR be increased. The presence of additional loss on the right side has been more clearly illustrated by the CFD. In comparison between EFD and CFD for the whole cases, the centre of the first loss cores have been predicted approximately 25% higher in span direction. As discussed above, this core was probably associated by the passage vortex. Furthermore, the strength of the passage vortex is also depending on the vortical structures that coming from upstream such as horse-shoe vortex. Hence, differences of first core height in span direction could be considered due to the difference inlet boundary condition used in EFD and CFD. The higher velocity region close to the endwall by the CFD provided a higher flow momentum near the endwall region consequently increased the growth rate of the vortical structure in span direction.

In Fig. 9, the total pressure loss for baseline condition and for the two MFR cases, are provided to give information on the aerodynamic performance of the leakage ejection system. Total pressure loss distributions confirm that the region affected by secondary flows increases in spanwise direction for higher MFR cases. This is due to the lifted up of the total pressure loss core towards midspan, associated with the passage vortex at this region. The loss distribution based on predictions were higher for the whole case. However, the distribution also presented a similar trend with the EFD. The higher the MFR, the higher losses were provided in spanwise direction. As discussed above, this is might be due to the different

inlet profile was used in CFD prediction. Three dimensional flow streamlines illustrated by the CFD prediction are shown in Fig. 10. Predicted flow streamlines for baseline condition, MFR=1.2% and MFR=2.2% are shown in (a), (b) and (c), respectively. For baseline condition, the PS horse-shoe vortex and SS horse-shoe vortex could be observed. At blade downstream plane, the presence of passage vortex near the blade SS and a corner vortex at the bottom side of passage vortex were predicted. SS horse-shoe vortex seems not to be mixed out with the passage vortex and remains until blade downstream. However, upstream leakage ejection obviously affected the secondary flows structures starting from just downstream of the leakage slot. Cooling air ejection at this location influenced to the increased strength of the vortical structure at blade upstream. This influenced to the increased strength of the passage vortex at blade downstream for higher MFR case. The SS horse-shoe vortex seems to be mixed out with the large passage vortex at blade downstream.

CONCLUSIONS

The investigation of aerodynamics performance on turbine cascade endwall cooling by the influenced of upstream leakage flow have been done by measurements and also numerical simulation. Upstream leakage ejection obviously effected the secondary flow field. Ejected leakage flows caused the presence of additional losses close to the endwall region. As the MFR increases, this loss region became wider in spanwise direction due to the increase strength of vortical structures near the endwall. This was also proved by the increased strength of the vortical structure at blade downstream to produce a large passage vortex for higher MFR case. Furthermore, the shape and position of first loss core were changed and moved towards midspan. The second loss core which is close to endwall

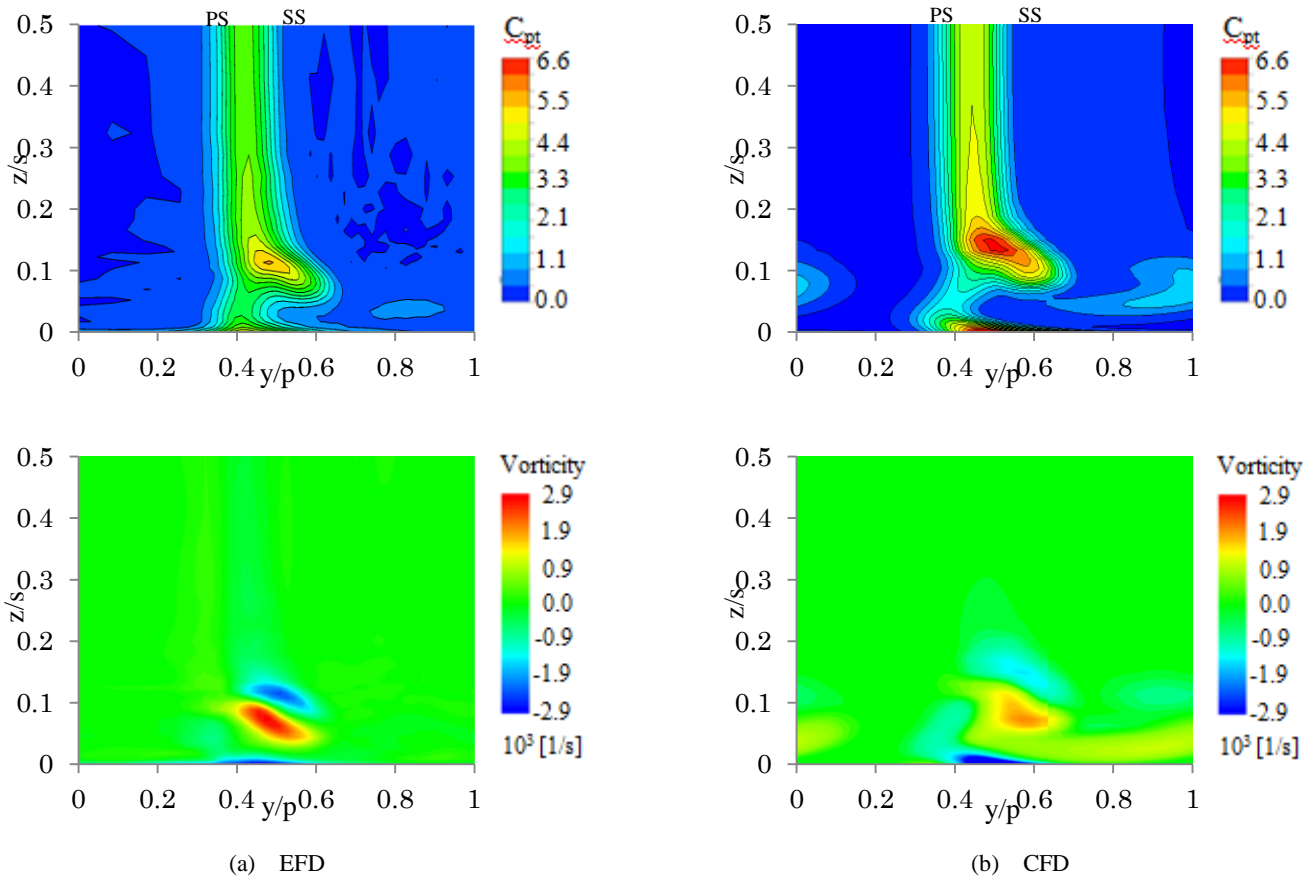


Fig. 7 MFR=1.2% - Total pressure loss and vorticity

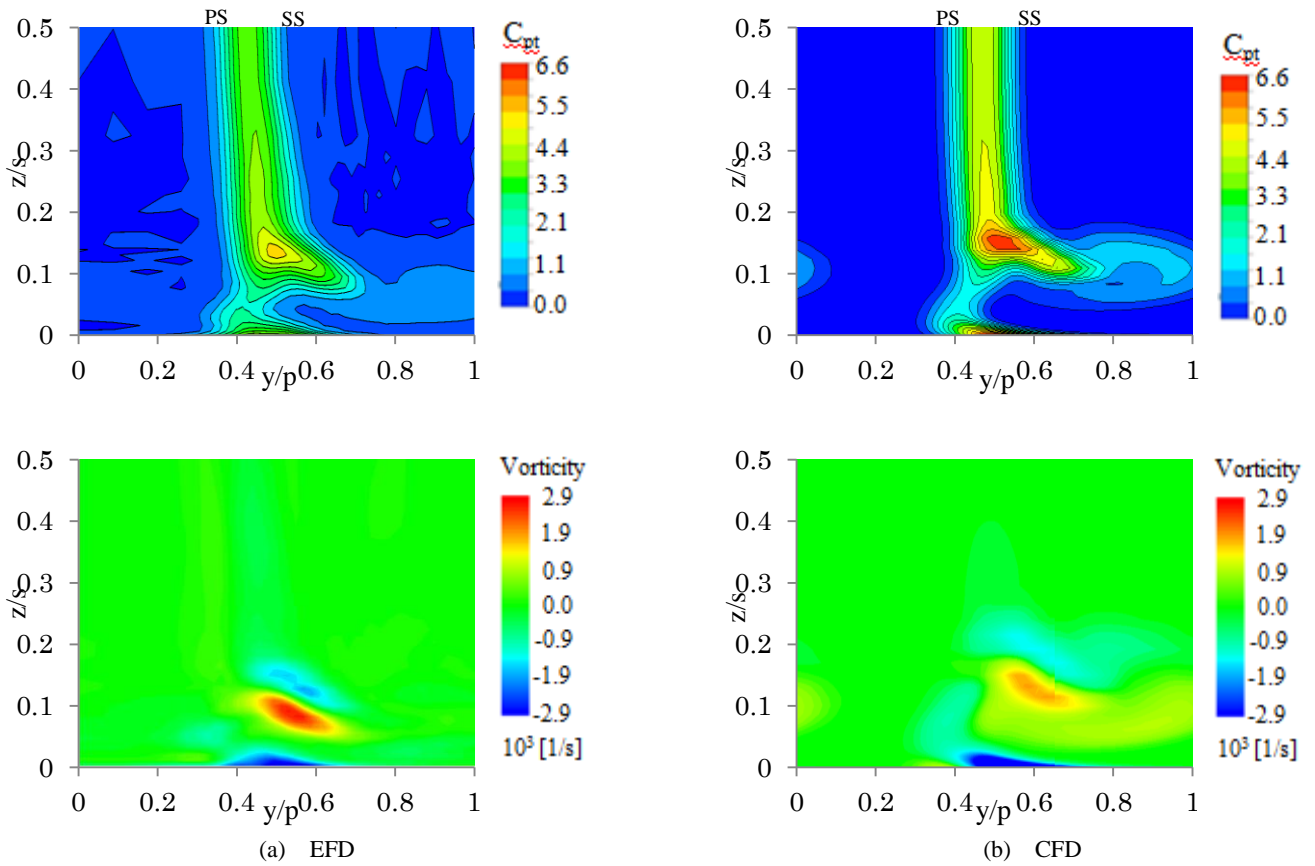


Fig. 8 MFR=2.4% - Total pressure loss and vorticity

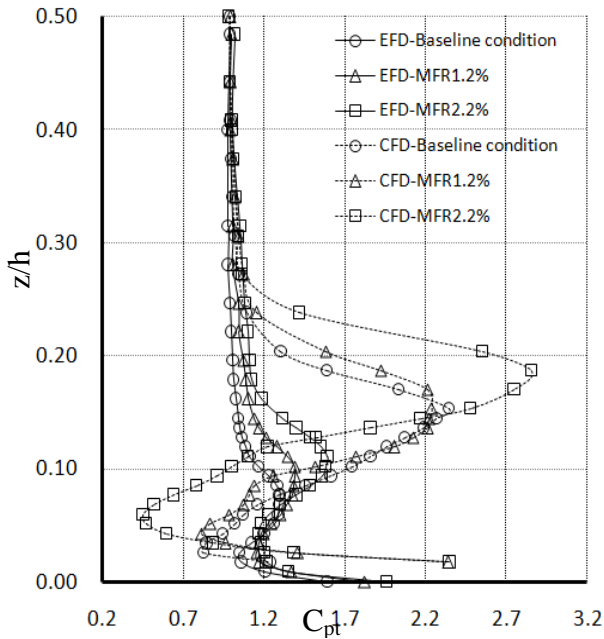


Fig. 9 Normalized total pressure loss

was also increased the region radially after the ejection and the highest MFR of 2.1% provided wider second core region. A numerical simulations based on SST model overpredicted losses at blade downstream approximately 20-30% compared with experimental. Even though similar trends of contours were shown in predicting the effect of leakage ejection, the centers of the core region influenced by the passage were higher 30% in spanwise direction for the whole case. The different inlet condition used in prediction compared with experimental was being considered as the main reason CFD could not properly predict the growth rate of the vortical structures at blade downstream. Furthermore, a numerical simulation allows the authors to have detail information on the interaction of the ejected cooling air with the main stream which could not merely be obtained by experimentally.

Acknowledgement

The authors grateful acknowledgement to Hitachi Corporation for the financial support in this study.

References

Blair, M.F., 1974, "An Experimental Study of Heat Transfer and Film Cooling on Large-Scale Turbine Endwalls", *ASME Journal of Heat Transfer*, **96**, pp. 524-529.

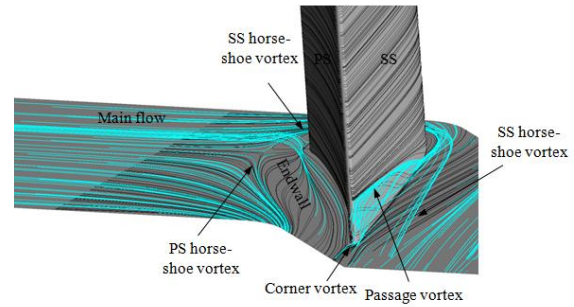
Goldstein, R. J. and Spores, R. A.; 1988 "Turbulent Transport on the Endwall in the Region Between Adjacent Turbine Blades", *ASME Journal of Heat Transfer*, Vol. 110, pp. 862-869.

H.J.Rehder, A.Dannhauer, Experimental Investigation of Turbine Leakage Flows on the Three-Dimensional Flow Field and Endwall Heat Transfer, *Journal of Turbomach*, Vol.129, 2007, pp. 608-618

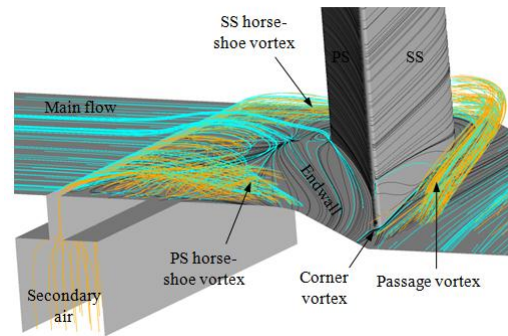
J.D.Piggush, T.W.Simon Heat Transfer Measurements in a First-Stage Nozzle Cascade Having Endwall Contouring Misalignment and Leakage Studies, *Transaction of ASME* Vol.129, 2007, pp. 782-790

Kang, M. B. and Thole, K.A.; 1999 "Flowfield Measurements in the Endwall Region of a Stator Vane", *ASME Paper No. 99-GT-188*, *ASME Journal of Turbomachinery*, Vol. 122, pp. 255-262

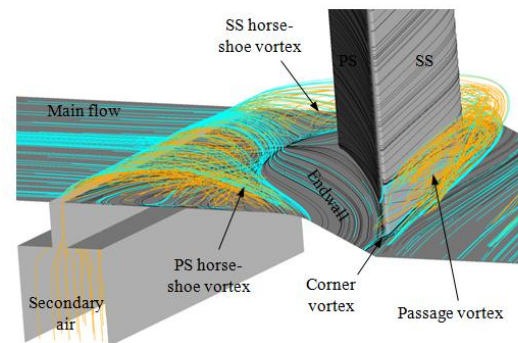
Kost, F., and Mullaert, A., 2006. "Migration of Film-Coolant from Slot and Hole Ejection at a Turbine Vane Endwall". *GT2006-90355*



(a) Baseline condition



(b) MFR=1.2%



(c) MFR=2.2%

Fig.10 Predicted 3D flow streamlines for each case

Kost, F., and Nicklas, M., 2001. "Film-Cooled Turbine Endwall in a Transonic Flow Field: Part I - Aerodynamic Measurements," *ASME J Turbomach* **123**, pp. 709-719.

Langston, L. S., Nice, M. L. and Hooper, R. M.; 1977 "Three-Dimensional Flow Within a Turbine Cascade Passage", *ASME Paper No. 76-GT-50*, *ASME Journal of Engineering for Power*, Vol. 99, pp. 21-28.

Sieverding, C. H.; 1984 "Recent Progress in the Understanding of Basic Aspects of Secondary Flows in Turbine Blade Passages", *ASME Paper No. 84-GT-78*, *ASME Journal of Engineering for Gas Turbines and Power*, Vol. 107, pp. 248-257.

S.P.Lynch, K.A.Thole, The Effect of Combustor-Turbine Interface Gap Leakage on the Endwall Heat Transfer for a Nozzle Guide Vane, *Journal of Turbomach*, Vol.130, 2008, pp041019-1-041019-10

Takeishi, K., Matsuura, M., Aoki, S. and Sato, T.; 1990 "An Experimental Study of Heat Transfer and Film Cooling on Low Aspect Ratio Turbine Nozzles", *ASME Paper No. 89-GT-187*, *ASME*

Journal of Turbomachinery, Vol. 112, pp. 488-496.

Wang, H. P., Olson, S. J., Goldstein, R. J. and Eckert, E. R. G.;
1995 "Flow Visualisation in a Linear Turbine Cascade of High
Performance Turbine Blades", *ASME Paper No. 95-GT-7, Houston,
Texas*